HYDROPHONE-BASED MONITORING OF BOAT TRAFFIC AND RESULTING AMBIENT NOISE

Sharmi Shah
MIT Department of Mechanical Engineering
Cambridge, MA, USA

ABSTRACT

To test the feasibility of utilizing a single hydrophone as a monitoring system for anthropogenic sounds, ambient noise levels of the Charles River over a week were recorded. In addition to ambient noise, the specific acoustic signals of motorboats driving past a hydrophone at varying speeds were recorded and examined to determine whether additional river traffic information can be derived from such signals. Averages of recordings taken between 7am-7pm and 7pm-7am, were compared and showed a significant difference in ambient noise, while also indicating that noise levels were below fish-harming thresholds. Cross correlations between specific motorboat signals and ambient data, as well as analysis of Doppler shifts in spectrograms of motorboat speed tests suggest extracting traffic data via hydrophone implementation is possible. These results show that a single hydrophone may be used as a simple, low-cost, and versatile data collection tool for determining nearby river traffic characteristics.

Keywords: Charles River, Hydrophone, Motorboat, Doppler Shift, Anthropogenic Sounds

INTRODUCTION

Understanding the patterns of boat traffic and recreational activities on rivers is important as anthropogenic sounds (noise that humans put into water) and high amounts of boat traffic can have adverse effects on wildlife, including physiological changes and temporary hearing loss [1]. Extracting traffic and ambient noise characteristics about a river by measuring its underwater noise could offer many advantages, such as monitoring environmental impacts of river activities on wildlife. Previous studies have examined estimation methods to measure boat traffic in oceans via spectral analysis of underwater noise data collected from hydrophone arrays [2]. While these studies have developed a high-fidelity solution to monitoring boat traffic, whether data from a single hydrophone can perform a similar estimation has not been tested. A successful design of a low-cost one-hydrophone system to monitor the ambient noise of a river would allow for an affordable and simple way to monitor boat traffic patterns and evaluate if underwater noise levels are suitable for animal life.

In order to test the feasibility of a single hydrophone monitoring system for anthropogenic sounds, ambient sound levels and specific acoustic signals of motorboats on the Charles River were examined. A hydrophone was placed in the Charles River near the MIT Sailing Pavilion to record underwater sounds for a week. Daily averages of recordings taken between 7am-7pm and 7pm-7am were compared to identify differences in the underwater acoustic environment between the day and night within all frequencies as well as within frequencies fish are sensitive to. After ambient data collection, a motorboat was driven at varying speeds past the stationary hydrophone. Cross correlations between motorboat signals and the week-long ambient data recordings were performed to identify the number of boats that passed the hydrophone daily. The acoustic data was also represented as spectrograms and examined for various phenomena, including a Doppler shift. The accuracy of using the Doppler shift as a speed estimation method for motorboats via spectral analysis of data collected with a single hydrophone was evaluated. This experiment may be valuable to the design of low-cost underwater noise monitoring systems which can be deployed to characterize motorboat traffic and evaluate the safety of an underwater environment for fish.

BACKGROUND

HYDROPHONES

A hydrophone is an underwater microphone designed to detect underwater noise. Similar to a microphone, a typical hydrophone operates by converting a sound wave, or changes in pressure, to an electrical signal. Piezoelectric materials are commonly used in hydrophones because they respond to changes in pressure or exerted mechanical energy with a proportional change in voltage [3]. A hydrophone can detect sounds in air, however its acoustic

impedance is calibrated for sound detection underwater. An omnidirectional hydrophone is one that will pick up sounds equally from all directions. An omnidirectional hydrophone is ideal to use for a single-hydrophone river monitoring system as it will allow the hydrophone to capture data from traffic surrounding the hydrophone.

AMBIENT NOISE IN RIVERS

Ambient noise in rivers originates from two main sources: sounds from natural processes (e.g. wind, precipitation) and anthropogenic sounds (e.g. boats, human activities) [4]. Motorboats are one common example of an anthropogenic sound that contributes to underwater ambient sounds. Vibrations from the engines of a vessel like a motorboat are related to the firing rates of the engines which vary depending on the engine's size. Larger engines produce lower frequency vibrations (<1Hz-10Hz) while smaller engines produce higher frequency vibrations (10Hz-200Hz) [5].

Previous research on environmental monitoring of large rivers shows that anthropogenic noises, including traffic on the riverbanks, affects underwater ambient noise levels [4]. Another study has demonstrated correlations between underwater acoustics and the characteristics of the corresponding riverbed [6]. Yet another study on the Hudson River indicated that boating activities increased sound levels during the day, and especially over the weekends [7]. It remains to be seen whether a one-hydrophone setup can demonstrate similar environmental monitoring by extracting characteristics about underwater sound level differences during different parts of the day and week.

ENVIRONMENTAL IMPACTS OF HIGH AMBIENT SOUND LEVELS

Many vertebrates living underwater, including fish, use sound as an integral part of communicating, and sensing their environment. For instance, determining the direction from which a sound came can help them detect potential prey or escape predators. Although long term rises in ambient sound levels are not likely to result in any dramatic consequences such as death, they could produce long-term hearing loss, behavioral effects, or auditory masking [8].

Auditory masking is a phenomenon that occurs when anthropogenic sounds are within the frequency range of what fish can hear [1]. Figure 1 depicts typical frequencies and corresponding intensities that some species of fish are sensitive to. Typical fish hearing sensitivities fall between 50Hz and 450Hz [1]. The presence of other sounds in these ranges provide difficulty for the fish in detecting biologically relevant sounds such as sounds from a predator. Motorboats specifically, have been shown to affect the routine swimming and escape response of fish [9]. The U.S. National Marine Service currently uses 150 dB re 1 µPa (150 dB with reference to 1 micro-Pascal) as the threshold sound pressure that may result in behavioral changes in fish [1]. For reference, being next to a jackhammer or lawn mower is 125 dB re 1 µPa. A one-hydrophone monitoring system could allow for a simple way to test whether auditory masking is present in smaller bodies of water such as a river as well as if ambient sound levels surpass the fish harming sound pressure threshold.

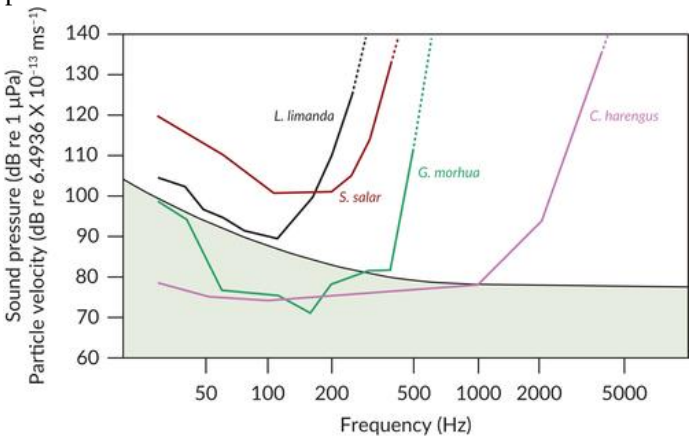

Figure 1: Fish hearing sensitivity responses to pure tone stimuli under open-sea conditions for four different species. Reference level of ambient is seen in the shaded curve [10]. This information provides a baseline for my work on evaluating the safety of an underwater acoustic environment for fish.

SOUND PROPOGATION AND REFLECTION IN WATER

Sound propagates via vibrations and the speed of these vibrations depends on the density of the medium it is traveling through. In freshwater, the speed of sound is about 1500 m/s [11]. Sound in the ocean and large rivers can be received via multiple paths as a result of reflections and scattering. If the river-surface were perfectly smooth, it would form an almost perfect reflector of sound. However, if the surface of the river is not fairly smooth, then there will be an interference pattern created by the different paths represented in Figure 2. If the signals coming from these paths are incoherent, meaning they are out of phase, they will interfere and create nulls, or spaces of no amplitude (due to destructive interference) [12].

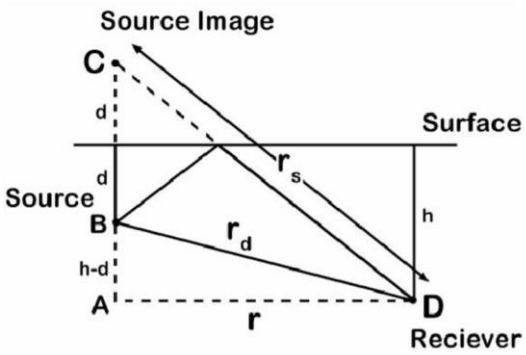

Figure 2: Geometry of surface interference with r_s = surface reflection ray length and r_d= direct ray length [12]. The surface reflection takes longer to reach the receiver than the direct ray meaning there will be interference of the two rays at the receiver.

As a sound source travels in the water, its sound will be nulled by (or destructively interfere with) the surface reflection at particular locations. This is known as Lloyd's mirror interference pattern, which can be easily visualized in a spectrogram. A spectrogram is a visual representation of frequencies of a signal as they vary with time. Figure 3 shows a broadband spectrogram of an underwater, sound-emitting target. The Lloyd's mirror interference pattern is indicated by the white hyperbolic shapes, otherwise known as "striations". The white spaces indicate nulls, where the direct ray and reflected ray interfere.

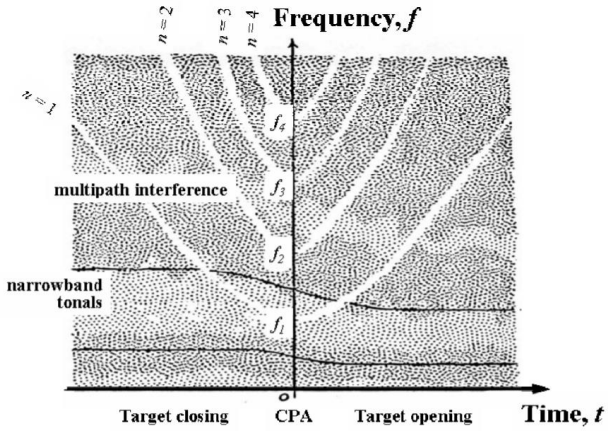

Figure 3: Frequency versus time representation of data taken by a hydrophone of a moving target passing the hydrophone [12]. The white hyperbolas indicate Lloyd's mirror interference pattern. The center of the horizontal axis shows time t=0, when the target passes right by the hydrophone, otherwise known as the CPA (closest point of approach). Before t=0, the target is still approaching the hydrophone and after t=0, the target has departed the hydrophone. The two black lines horizontally spanning the graph are narrowband tonals which represent frequencies emitted by the target that change in frequency as they pass through the CPA. The frequency shift in the narrowband tonals can be used to measure the speed of the target.

An important characteristic of the hyperbolic shapes is the closest point of approach (CPA) which occurs at t=0. This is where the sound source was closest to the recording instrument and also where the hyperbolic shapes have their line of symmetry.

DOPPLER SHIFT AND SIMILAR EXPERIMENTS

The Doppler effect is a phenomenon which states that there is a change in frequency when there is relative motion between an observer and a target (Figure 4). The Doppler shift is frequently used to track ships or other targets in the water as well as a method to compute a target's closest point of approach (CPA) [13].This can often be done via a spectrogram of the sound data. Figure 4 shows narrowband tonals that change in frequency as they pass through the CPA. The shift in frequency visible in the spectrogram is a result of the Doppler shift. The frequency values from the spectrogram can be extracted and used to calculate speed of the sound source using the following set of equations:

$$f_o = \frac{f_{upper} + f_{lower}}{2} \quad (1.1)$$

$$\Delta f = f_{upper} - f_{lower} = f_o \frac{v}{c} \quad (1.2)$$

$$v = c \frac{\Delta f}{f_o} \quad (1.3)$$

where f_{upper} is the maximum closing frequency (left of CPA), f_{lower} is the minimum opening frequency (right of CPA), $c = 1500 \frac{m}{s}$ is the speed of sound in water, and v is the speed of the sound source.

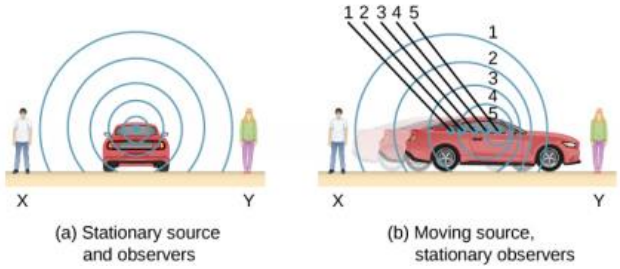

Figure 4: Frequency versus time representation of data taken by a hydrophone of a moving target passing the hydrophone [12]. The white hyperbolas indicate Lloyd's mirror interference pattern. The center of the horizontal

There are many previous studies that have demonstrated tracking ships via spectral analysis. One such study demonstrated calculation of target location range and speed at a target's CPA in the ocean via a hydrophone setup [12]. Another study utilized four hydrophones to

develop a navigation method by analyzing an underwater object with an attached transmitter emitting a constant signal [14]. Although these studies have deeply explored the use of the Doppler shift to analyze trajectories of moving objects in the ocean from multi-hydrophone data, they have not extensively studied using this phenomenon to measure boat traffic speeds via a single hydrophone setup in a river.

EXPERIMENTAL DESIGN

A hydrophone connected to a data acquisition system was deployed off the MIT Sailing Pavilion dock into the Charles River. Sound data was collected for two weeks. Then, specific signals of a motorboat passing by the dock were recorded. Finally, acoustic signals of motorboats at varying speeds as they passed by the hydrophone were recorded.

HYDROPHONE CALIRATION

A CAL73 calibrator was used to calibrate the hydrophone. The CAL73 was placed at the 114dB setting and the hydrophone captured the emitted sound. Thereafter, the following set of equations were used to acquire a calibration constant:

$$P_{rms} = P_{ref} 10^{\left(\frac{SPL}{20}\right)} \quad (2.1)$$

$$K = \frac{P_{rms}}{\sigma_{mic}} \quad (2.2)$$

where $P_{ref} = 20\mu Pa$, $SPL = 140dB$, and the standard deviation of the hydrophone recording, σ_{mic}=0.1961Pa. The resulting calibration constant, $K = 51.11$. The arbitrary units given by the hydrophone output were converted to dB re 1 μPa via:

$$SPL(dB) \equiv 20log_{10}\left(\frac{P_{rms}}{P_{ref}}\right) \quad (3.1)$$

$$P_{rms} = KP_{uncalibrated} \quad (3.2)$$

where $P_{ref} = 1\mu Pa$, $K = 51.11$, and $P_{uncalibrated}$ is the value the hydrophone collects in arbitrary units.

HYDROPHONE CONFIGURATION

In order to record sound data underwater, an H2A hydrophone, which measures acoustic pressure in arbitrary units (which can be converted to Pa via calibration results), was configured with a Raspberry Pi 4B. The Raspberry Pi was connected to an Adafruit USB audio adapter which was then connected to the audio jack of the hydrophone. In order to operate the Raspberry Pi with the hydrophone, several configuration and logging shell scripts were written. The Raspberry Pi, hydrophone and power cord were all placed in a waterproof box on the MIT Sailing Pavilion Dock (Figure 5). The location of the MIT Sailing Pavilion in relation to the Charles River is indicated in Figure 6.

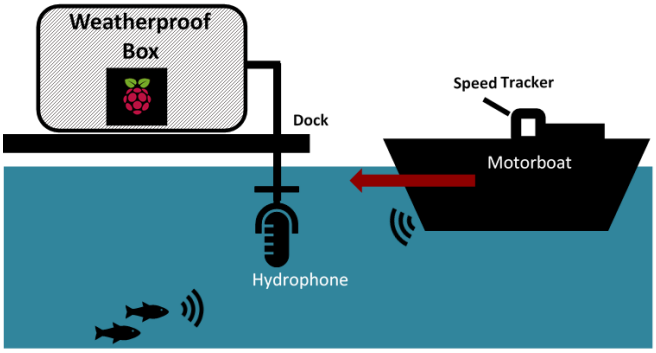

Figure 5: A block diagram of the experimental setup with the data acquisition system. The black dotted-lined box indicates the parts of the setup that were placed inside of the weatherproof box. The hydrophone wire was placed 5 ft in the water and recorded sounds for all phases of the experiment.

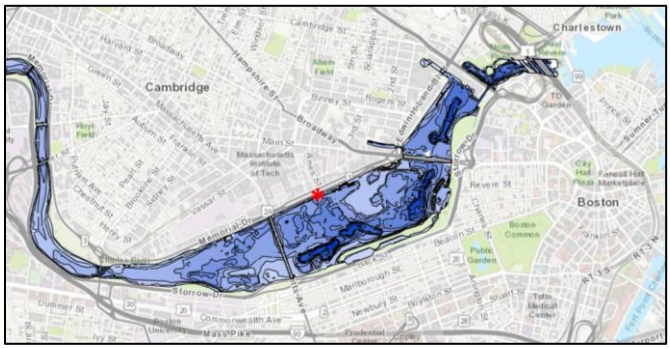

Figure 6: Aerial view of the Charles River where darker blues represent deeper parts of the river. The red star indicates the location of the hydrophone and the MIT Sailing Pavilion in reference to the ocean and other parts of Massachusetts [15].

AMBIENT DATA EXPERIMENTAL EXECUTION AND ANALYSIS METHODOLOGY: PHASE I

The hydrophone recorded underwater sounds of the river for two weeks at a sampling frequency of 44.1 kHz. The hydrophone was placed 5 feet deep in the water off the side of the Sailing Pavilion dock (Figure 5) and the Raspberry Pi was set to record for 5 minutes, rest for 5 minutes, and then repeat that process by starting to record again. This way, one 5-minute section was recorded every 10 minutes, totaling 12 hours of data collected daily. Data was offloaded from the Raspberry Pi about every two days.

Only the first week of data was used for analysis, as the second week was biased from rainy weather and the Head of the Charles competition. The 5-minute audio segments from 7am-7pm and 7pm-7am were aligned and

combined separately for each day over the first week using Audacity. In order to identify the impact of river activity on frequencies within fish hearing sensitivity, average amplitudes of hydrophone data within the 50Hz-450Hz band were extracted for each segment of time using (4.1).

$$\frac{1}{450-50}\int_{50Hz}^{450Hz} FFT(segment)df \qquad (4.1)$$

The integral bounds represent typical fish hearing sensitivities and each FFT(segment) indicates the Fast Fourier Transform of each day/night section over a week.

TRAFFIC DATA EXPERIMENTAL EXECUTION AND ANALYSIS METHODOLOGY: PHASE II

To acquire a standard driving motorboat underwater acoustic sample, a Carolina Skiff motorboat with a 25 HP Yamaha engine (Figure 7a) located near the hydrophone was turned on, driven away, and driven back to its resting location. This trial was done twice as the hydrophone recorded this process. Groups of three 5-minute raw time signals (15 minutes total) during open Sailing Pavilion hours (12pm-7pm) from the first week of ambient data collection were cross correlated with an acoustic sample of the Carolina Skiff. Cross correlations from the week were visually scanned for peaks, where each peak would represent a motorboat event.

AMBIENT DATA EXPERIMENTAL EXECUTION AND ANALYSIS METHODOLOGY: PHASE III

Next, a set of trials were performed with a Tornado Rigid Inflatable motorboat (Figure 7b) with a 60 HP Yamaha engine driven at various speeds from 2m/s – 5m/s past the hydrophone. An app, iSailGPS, was used to track the speed of the motorboat during trials. The hydrophone was moved to a location in front of the MIT Sailing Pavilion for this set of trials. An employee of the Sailing Pavilion drove the motorboat beginning roughly 15m before the location of the hydrophone and about 15m past along the dock. The boat was driven from the same side of the hydrophone every trial.

Spectrograms of motorboat speed trials were taken with a 16384 Hann window (for higher frequency resolution) using MATLAB. Doppler shifts of narrowband tonals and striations similar to those seen in Figure 3 were visually identified in the experimental data spectrograms. Calculations for speeds based on Doppler shifts were calculated using equations 1.1-1.3 for each trial.

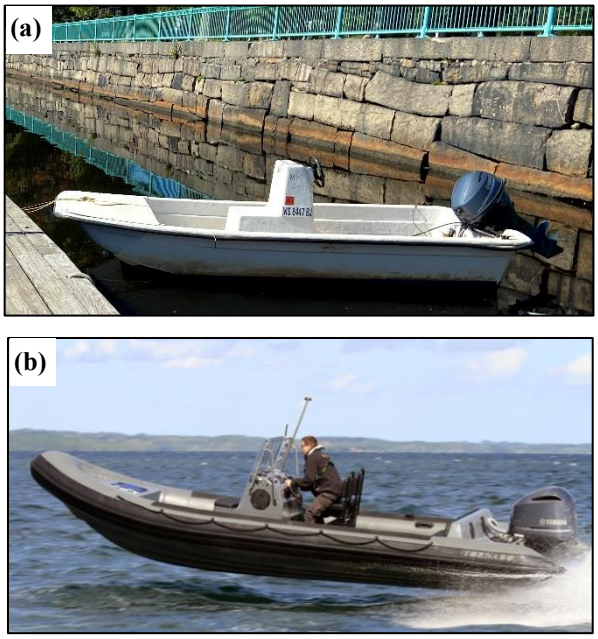

Figure 7: The two images are motorboats that were used during experimental trials. (a) Is a Carolina Skiff motorboat which was used during traffic data collection. (b) Is an example of a Tornado Rigid Inflatable motorboat. A similar motorboat was used for motorboat speed experimental trials.

RESULTS

The ambient sound levels during the day versus night of the Charles River were measured and compared for all recorded frequencies and frequencies within typical fish hearing sensitivities. Cross correlations of ambient sound levels with specific motorboat signals allowed for a method to identify motorboat traffic on the Charles. Spectrograms of motorboat acoustic signals at varying speeds were taken and important features such as striations and narrowband tonals (Figure 3) were identified. The frequency shift in the narrowband tonals was used to calculate a Doppler shifted speed via equations 1.1-1.3.

AMBIENT SOUND ANALYSIS

Representative data of perturbation pressure measured by the hydrophone for ambient data collection is shown in Figure 8. Data collected for each hour over one week was averaged to obtain average hourly amplitudes. The busiest hour of the day over the week, indicated by the greatest average perturbation pressure, was found to be 7pm with an average perturbation pressure of 0.664±0.045 Pa. The quiestest hour, indicated by the lowest average perturbation pressure over the week, was 11pm with an average perturbation pressure of 0.3996±0.0014Pa (Figure 9).

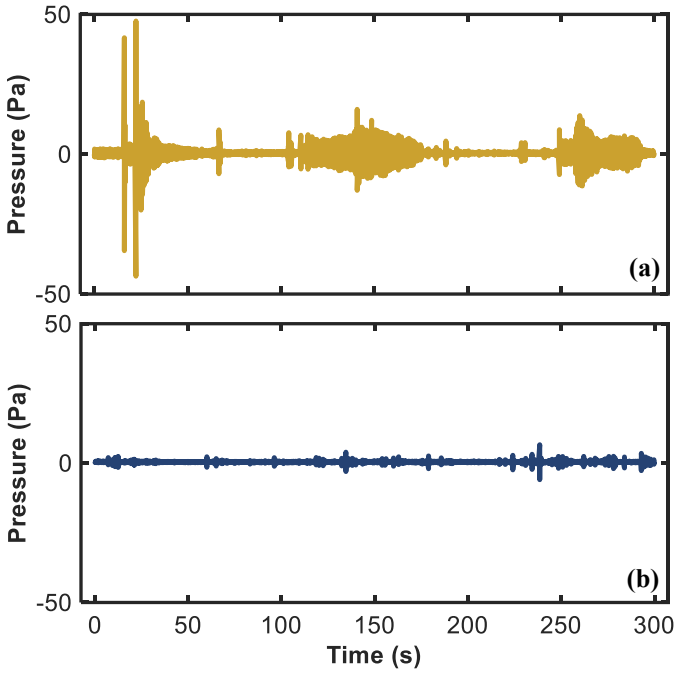

Figure 8: Time series of ambient hydrophone data taken on 10/03/2021 during the loudest hour from 7:10pm-7:15pm (a) and during the quietest hour from 11:10pm-11:15pm (b). At the particular interval of time shown in graph a, there were several disturbances, as indicated by the sections of greater amplitude.

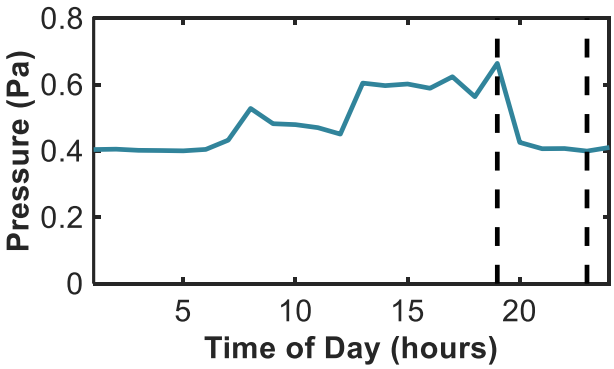

Figure 9: Measurements recorded by a hydrophone were averaged for each hour over one week. In the plot above, hour 1 represents averaged data from 12am-1am and hour 24 represents averaged data from 11pm-12am. There was a rise in activity during the middle of the day when compared to the early morning or late night. The greatest and lowest average amplitudes were at 7pm, with an average value of 0.664±0.045 Pa and 11pm, with an average value of 0.3996±0.0014Pa respectively. The dashed black lines indicate these maximum and minimum values. The shaded blue section depicts the open hours of the MIT Sailing Pavilion during which there are higher amplitudes of noise levels.

There is a visual difference in the amplitudes from the two samples of ambient acoustic data in Figure 8. One reason for this difference is motorboat usage. The three distinct sections of increased amplitude in Figure 8a are most likely a result of motorboats emitting sound underwater. Contrastingly, the evening does not see much activity, especially since the MIT Sailing Pavilion is closed by this point in the day. Figure 9 gives a broader perspective on the activity nearby the Sailing Pavilion over a day. When the Sailing Pavilion is open, there are higher noise levels in the Charles, likely due to the increase in motorboat activity. Other recreational activities such as sailing and kayaking may also contribute to the increased noise, however they do not emit as loud of an acoustic signal as motors on a motorboat do.

To further investigate the relationship between time of day and ambient noise levels in the river, t-tests were conducted between hydrophone data from daylight hours for each day versus night hours (Figure 10a). There was a statistically significant difference at the 95% confidence interval, showing that the ambient noise levels of the Charles increase during the day, which is reasonable, as more activity occurs on the Charles during the day. If there is a difference in activity between day and night, is there a similar difference in activity between the weekdays versus the weekends, when people may have more leisure time? A t-test assuming unequal variances was conducted on weekday vs weekend data during open Sailing Pavilion hours (12pm-7pm) and no statistical significance was found between the two sets of data (Figure 10b).

Although the ambient sound levels significantly vary between day and night, there is no apparent difference between the sound levels during the week versus the weekend over open Sailing Pavilion hours. The difference in ambient sound levels between day and night agrees with the results of the studies done on the Hudson River, stating that boating activities increase underwater sound levels during the day [7]. However, these results disagree with the same study in terms of increased activity during the weekend. There is a possibility that there was less than typical activity on the Charles due to some event. More weeks of sound data from the river would have to be analyzed to clarify whether the insignificant difference between sound levels from the weekdays versus the weekend is an anomaly or a pattern. Regardless, the hydrophone setup was able to successfully determine the daily trends in activity on the Charles over a week. This capability may be useful in characterizing the patterns of local activity in a variety of marine environments.

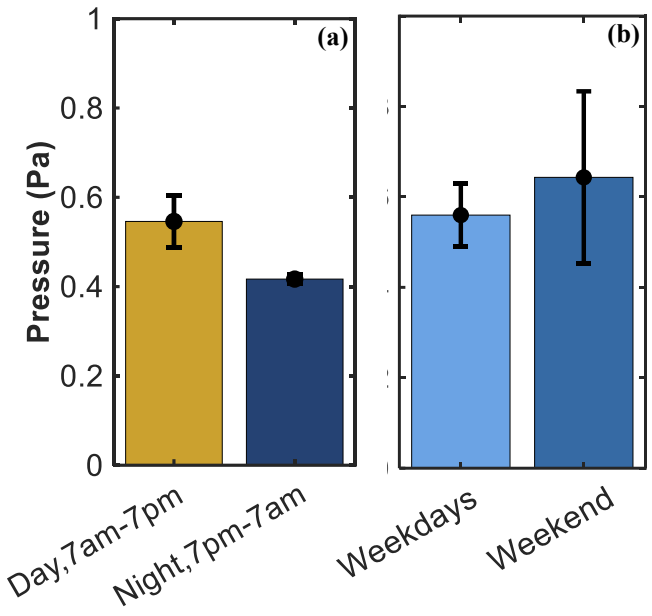

Figure 10: (a) Hydrophone data was averaged over daylight hours and night hours for each day of the week. The amplitude of perturbation pressure for the daytime is 0.542±0.056 Pa and is significantly greater than the pressure for the night over a week: 0.416±0.011 Pa (p=0.00012). This reasonably indicates that ambient sound levels of the Charles increase during the day when the Sailing Pavilion is more active. Error bars indicate the 95% confidence interval. (b) Hydrophone data was averaged over MIT Sailing Pavilion open hours, 12pm-7pm, for each day. Weekday averages were compared with weekend averages and no statistical significance was present between the weekday vs the weekend. Error bars indicate the 95% confidence interval.

The effects of increased activity during the day and on auditory masking was evaluated by analyzing sound levels of the river within typical fish hearing sensitivities (50Hz-450Hz) between the day and night. The frequency content of the Charles during a segment during the day versus evening are shown in Figure 10. The frequency spectra indicate that sound levels corresponding to frequencies within the fish hearing sensitivity range may be greater during the day.

A t-test was conducted to compare the average amplitudes of sound levels within the 50Hz-450Hz band, computed via equation 4.1, during the day versus night (Figure 12). There was no significant difference at the 95% confidence interval between the average amplitude during the day versus the evening within the 50Hz-450Hz band. This shows that the increase in activity on the Charles river does not specifically affect the frequencies that are relevant to fish hearing.

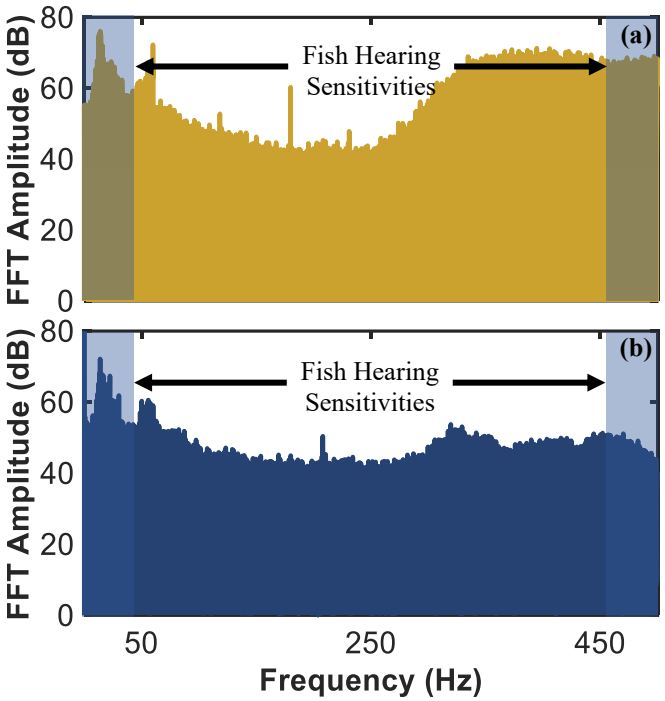

Figure 11: The frequency spectrum of hydrophone data taken on 09/30/2021 from 12:40-12:45pm (a) and from 11:40-11:45pm (b). There is a visible increase in amplitude within the range of typical fish hearing sensitivities, indicated by the arrows, during the sample of data during the day versus the evening.

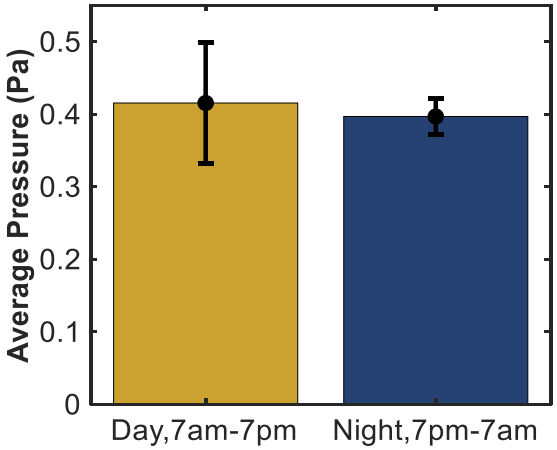

Figure 12: Hydrophone data within 50Hz-450Hz was averaged over daylight hours and night hours for each day of the week. The amplitude of perturbation pressure for the daytime is 0.416±0.084 Pa and is not significantly greater than the pressure for the night over a week: 0.397±0.025. It cannot be conclusively said that the river activity during the day affects fish hearing sensitivities. Error bars indicate the 95% confidence interval.

The average amplitude during the day (0.416±0.084 Pa) represented in decibels is about -7.6181±(-22) dB re 1µPa which is much less than 150 dB re 1 µPa: the U.S. National Marine Service's threshold for harmful sound levels for fish [8]. This shows that the Charles River is a safe acoustic environment for fish to survive in. The negligible impact of the increase in activity during the day on sound levels within fish hearing sensitivities was unexpected, especially considering that there was a significant difference when all frequencies were analyzed. It is plausible that averaging quiet sections with sections containing motorboat events failed to capture the effects of loud sounds on the fish hearing sensitivity frequency band. Further testing on average amplitudes spanning fish hearing sensitivities specifically when motorboats are in use may shed insight on whether the noise emitted by motorboats results in auditory masking. A similar analysis can be performed using measurements from a single hydrophone to evaluate the general suitability of other aquatic environments for marine life.

TRAFFIC DATA ANALYSIS

Segments of representative data from ambient acoustic data collection of a motorboat passing near the hydrophone and when there was no motorboat nearby the hydrophone are seen in Figure 13a-b. The time series with a "motorboat event" has a section of much greater amplitude than the time series without the "motorboat event" due to the emission of sound by the motorboat. A signal of a specific motorboat signal is also seen in Figure 13c, which has high amplitudes due to the motorboat's acoustic emissions.

The time series of the motorboat's acoustic signal indicates that the hydrophone is susceptible to saturation when the motorboat is too close to the recording device. The only evidence of similarity between plots 12b and 12c are the increased amplitudes compared to plot 12a. Cross correlating the specific motorboat signal, 12c, with the ambient data collected over a week may be able to indicate when a motorboat passed by the hydrophone versus when they were no motorboats around the hydrophone.

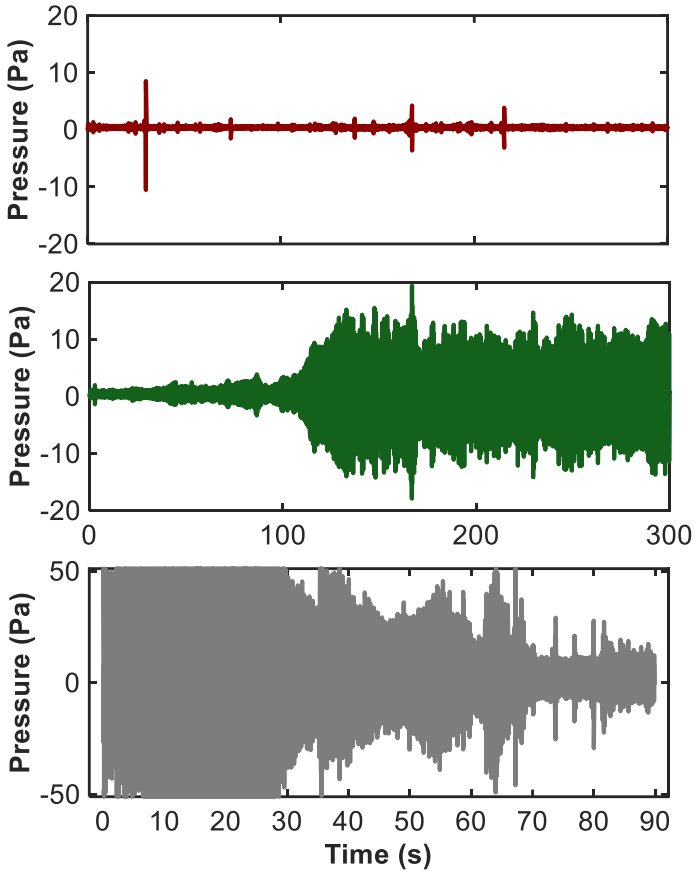

Figure 12: Recordings of ambient data in the Charles were taken and are represented in graphs (a) and (b). The data in (a) is a time series of a section of ambient data from 9/30/2021 at 12:30pm and indicates the type of data typically seen when there no motorboat. The data in (b), taken at 12:40pm of the same day, shows a motorboat traveling near the location of the hydrophone, which increases the amplitude of the recorded signal. Finally (c), shows the specific acoustic signal (not from ambient data collection) of the same motorboat driving by the hydrophone.

Cross correlations were performed on ambient sound data over open MIT Sailing Pavilion hours (12pm-7pm). The cross correlations generated graphs with peaks, indicating when a motorboat was being driven (Figure 14). These graphs have sharp rise times and falls times because the signal from driving the motorboat is shorter than the data being compared to it, so it has been padded with zeros and the correlation at these zeros is zero. The graph window chosen in the cross correlation focuses on the relevant parts of the comparison.

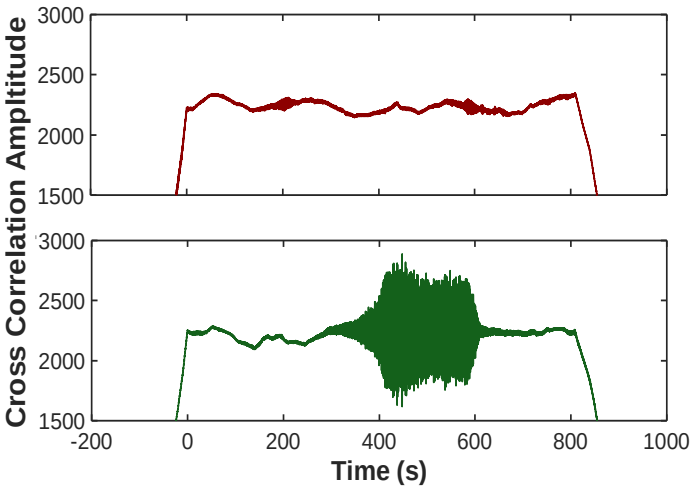

Figure 14: Cross correlations of time signals from 12:00pm-12:30pm (a) and 12:30pm-1:00pm (b) on 09/30/2021 with recorded motorboat signal. Graph (a) is the cross correlation of graphs 12a and 12c. Although graph (a) has some peaks, these are the periodic sounds of water that correlate between all signals. These mild peaks are therefore not considered in the tabulation of motorboat traffic. Graph (b) is the cross correlation of plots 12b and 12c. The large peak in graph (b) indicates that there was an occurrence of a motorboat near the hydrophone around 12:40pm which is supported by plot 12b.

Although the time series in Figure 13 indicates an acoustic event occurrence, Figure 14 is more thorough in clarifying this event as a motorboat event due to the peak visible in its cross correlation. The cross correlations from each time segment were visually scanned for peaks similar to the one in graph 13b. The results were tabulated and are represented in Figure 15.

The bar graph shows a lack of activity on Sunday and Monday -- perhaps the MIT Sailing Pavilion was less active on those days. The decrease in motorboat activity from Saturday to Sunday also explains the large variance in the weekend bar in Figure 10b. There may be multiple reasons for the decreased activity; one major factor that may have impacted boat traffic was the rainy weather on Monday. This data shows that tabulating peaks from cross correlations of motorboat signals is a viable method to study local motorboat traffic data from single hydrophone measurements. Further research into filtering algorithms that can count number of peaks from the noisy cross correlations in Figure 14 may offer a more efficient way to extract traffic data from hydrophone measurements.

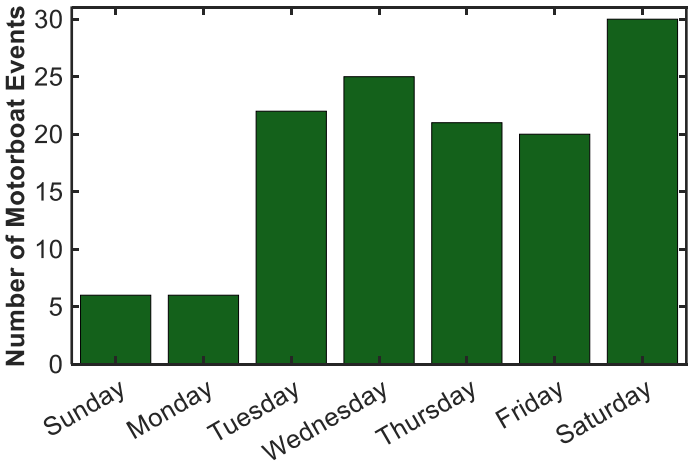

Figure 15: Tabulated peaks from cross correlations of motorboat signals with ambient data over a week. Saturday sees the greatest amount of traffic whereas Sunday and Monday are calmer days.

BOAT SPEED ANALYSIS

A representative signal from a motorboat speed trial is visible in Figure 16. Saturation effects are visible in the plot due to the close proximity of the motorboat to the hydrophone. Duration of a motorboat trial can be extracted from a time series such as the one in Figure 16 by looking at the section with greater amplitudes. However, spectrograms offer more insight into the behavior of the motorboat and its acoustic content.

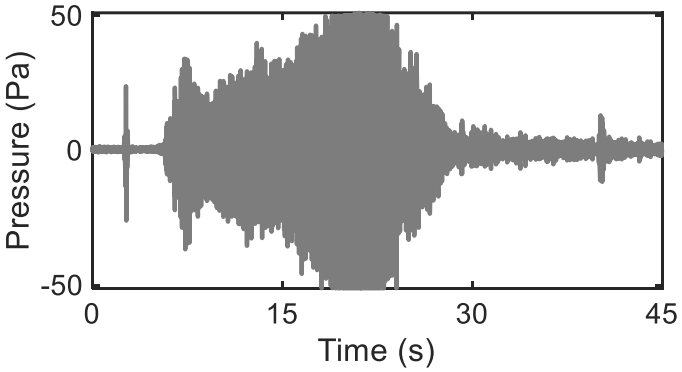

Figure 16: Recording of a motorboat driving at a measured speed of 3.5m/s represented as a time series with the hydrophone measuring perturbation pressure. The boat was active from around 5s-27s. Around 23 seconds, the motorboat drove right past the front of the hydrophone which can be deduced by the large amplitude and the fact that the 23 second mark acts as a line of symmetry about which the motorboat approached the hydrophone and then drove away.

Spectrograms of motorboat trials showed visual evidence of the striations and narrowband tonals depicted in Figure 3. Figure 17 shows a comparable spectrogram of a motorboat speed trial with tonals and hyperbolic striations.

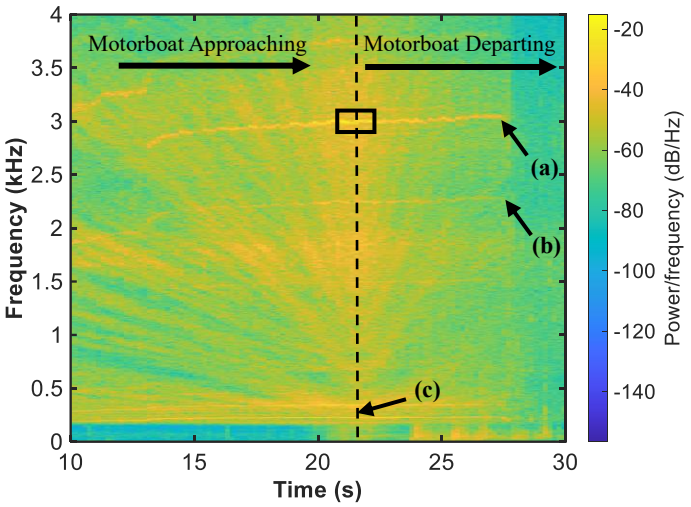

Figure 17: Spectrogram of motorboat traveling at an average speed of 3.5 m/s. Several narrowband tonals are visible in the spectrogram and two are pointed out by (a) and (b). The Doppler shift is not readily visible in this image but is boxed in the plot. A closer look at the boxed section, shown in Figure 19, makes it easier to visualize the shift. The slight upwards slope in the narrowband tonals is not a Doppler shift, but the result of variations in the motorboat's speed. The location of (c) shows the closest point of approach (CPA) which is the point where the motorboat passed right by the hydrophone. The hyperbolic shapes emerging about the dotted line are the striations, similar to those in Figure 3.

Comparing Figures 16 and 17 shows that the closest point of approach (CPA) is indicated in the time series as the point of highest amplitude about which the amplitudes symmetrically decrease and is indicated in the spectrogram as the symmetry line of a set of hyperbolas. Both of these plots show that the motorboat passed by the hydrophone around 23s. Spectrograms of all trials were taken, 3 of which are plotted in Figure 18. By focusing on the tonals, one can extract a speed by estimating the average frequency right before and right after the CPA and using equations 1.1-1.3.

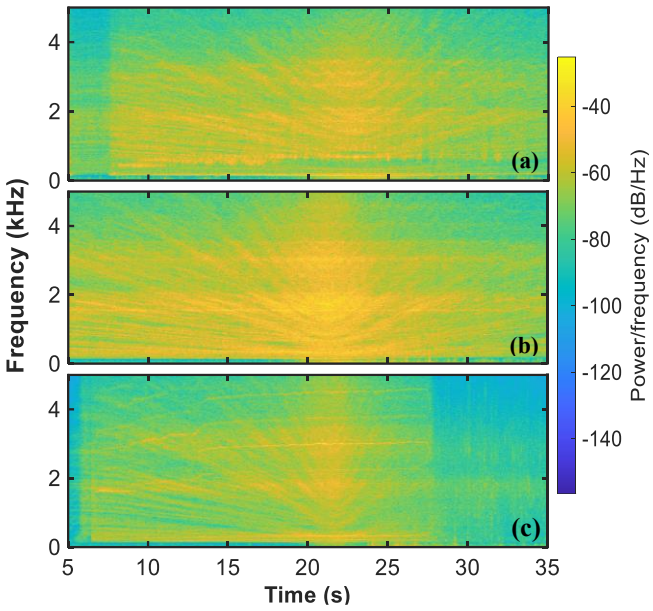

Figure 18: Spectrograms of motorboat speed trials for (a) 2.1 m/s (b) 2.8m/s and (c) 3.5m/s. The striations have increased slopes with increased speeds. The Doppler shift in the narrowband tonals (not visible here) is much more prominent in the trials with faster speeds because there is a greater shift in frequency.

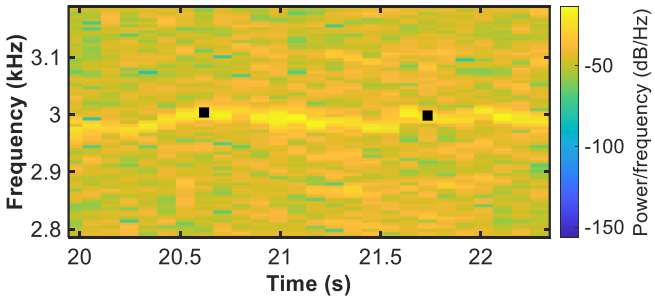

Figure 19: Expanded spectrogram for GPS speed of 3.5m/s (Figure 17). This is an expanded narrowband tonal which can be used to estimate the Doppler shift. The black points are placed as an average estimate of frequency band on either side of the shift. The maximum frequency was $f_u = 3003.8Hz$ and the minimum frequency was $f_l =$ 2998.5Hz. The calculated Doppler shift using equations (1.1-1.3) was 2.5m/s.

The spectrograms show that slope of the striations increase as the speed of the motorboat increases (Figure 18). These findings mirror those of a previous study on visualizing Doppler effects and striations due to Lloyd's interference [12]. The increased slope is a result of the motorboat covering more distance in the same amount of time.

There was some discrepancy between the Doppler shift measured value and the GPS measured value in Figure 19. To identify whether the Doppler shifts were able

to generally predict motorboat speeds, Doppler shifts were calculated for each trial. Table 1 lists all the GPS measured ground truth velocity values as well as the Doppler shift measured values. The GPS measured values and the Doppler shift measured values were plotted, along with the 95% confidence interval of the line of best fit for the plotted data in Figure 20. If the Doppler shift values were equal to the GPS measured values, the line of best fit would have a slope of 1. Therefore, a line with a slope of 1 (y=x) was also plotted and the Doppler shift method's efficacy was evaluated by checking if the line y=x was within the 95% confidence interval of the line of best fit, which had a slope of 0.97±0.11. The line y=x was indeed within the 95% confidence interval as seen in Figure 20, indicating that the Doppler shift method of calculating motorboat speeds is valid.

Figure 20 depicts that the Doppler shift method can be reasonably used to obtain values of motorboat speeds with data collected by a single hydrophone. As another check, a paired t-test between the two sets of data was completed and resulted in a $p<0.11$. Since the p-value was greater than 0.05, the GPS measured speed and Doppler measured speeds were statistically indistinguishable, showing again that the Doppler shift method is valid and that speeds of nearby motorboats can be evaluated using a single hydrophone.

Table 1: Recorded ground truth speeds and measured Doppler shift speeds for motorboat trials.

Trial	GPS Measured Speed (km/h)	GPS Measured Speed (m/s)	Doppler Measured Speed (m/s)
1	10.19	2.83	1.93
2	10.37	2.88	1.91
3	10.00	2.78	2.90
4	12.60	3.50	2.50
5	17.96	4.99	4.87
6	13.70	3.81	3.81
7	16.90	4.69	5.07
8	16.80	4.67	5.44
9	16.40	4.56	4.09
10	17.50	4.86	4.96

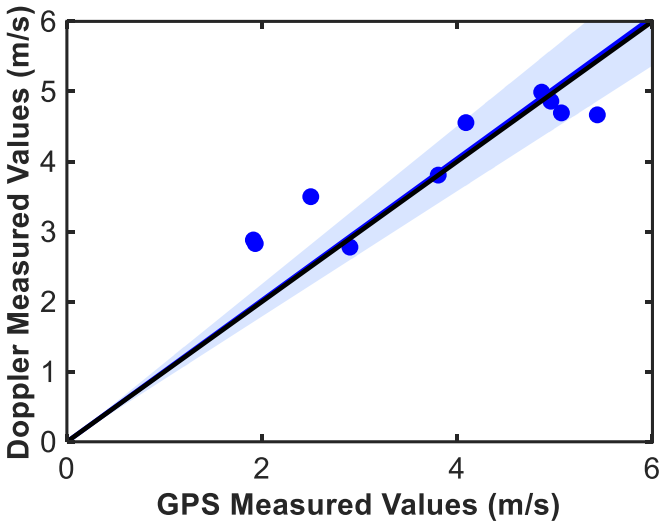

Figure 20: Speeds were calculated using the Doppler shifted frequencies from a spectrogram and compared with the ground truth GPS values. The blue points are the raw, measured values. The blue line represents the line of best fit with a slope of (0.97±0.11) and the shaded area represents its 95% confidence interval. The black line indicates the trend if the two sets of data were equal to one another, as they theoretically should be. The graph indicates that the black line is within the 95% confidence bounds and therefore the Doppler shift measured values are significantly similar to the GPS measured values and can be used as a method to predict motorboat speeds.

One limitation in this experiment was the resolution of the spectrogram. There were only so many discretized frequencies to pick from when identifying the frequency change at the CPA. Since the speeds were low, it was difficult to maintain precision in picking frequencies because the shift was so small that it occurred between 2-4 discretized frequencies. Increasing the window used to take the spectrogram would help, but comes at the expense of time resolution. In the future, faster speeds would be much better to test and may lead to better results.

CONCLUSIONS

A one-hydrophone monitoring setup was used to measure ambient sounds in the Charles River. The data suggests that the ambient sound levels of the Charles River are significantly increased during the day (0.542±0.056 Pa) when compared to the night (0.416±0.011 Pa), perhaps due to the increase in activity on the river during the day. Comparing day versus night sound levels within the fish hearing sensitivity frequency band suggests that there is no significant increase in sound levels within this band and therefore there is no evidence that sound emissions due to activities during the day affect fishes biologically.

Completing this analysis for the Charles River using data collected by a single hydrophone suggests that other aquatic environments can be investigated in a cost-effective manner for changes in ambient noise level patterns as well as for the suitability of noise levels for fish in the water. Further research is needed to identify whether these hydrophone measurements can determine if sound emissions from a specific motorboat can briefly create an environment with fish-harming sound levels.

In order to understand traffic data on the Charles, the measurements from the hydrophone setup were cross correlated with a specific signal of a motorboat passing by the hydrophone. This analysis demonstrated that motorboat events show up as peaks on these cross correlation graphs and these peaks can be tabulated to reasonably extract motorboat traffic data near the hydrophone. Motorboat traffic data calculated in this manner may also be able to indicate poor weather or other anomalies because people are less likely to partake in river activities on days with rainy or cold weather.

The same one-hydrophone setup was used to record motorboats at various speeds. Spectrograms of these measurements showed frequency shifts according to the Doppler effect. By measuring the frequency shift in the spectrogram, the speed of the motorboat could be reasonably predicted. However, another set of data collection with a higher sampling rate as well as faster motorboat speeds could allow for better spectrogram resolution and therefore produce more accurate results. Further analysis is required to fully understand the robustness of this method with data derived from a single hydrophone, especially with motorboats at farther distances.

Overall, this data suggests that measurements from a low-cost one-hydrophone setup can be used to reasonably obtain nearby river characteristics such as noise levels, boat traffic measurements, and speed of motorboats.

ACKNOWLEDGEMENTS

I would like to thank Professor Hughey and Professor Peacock for all of their help through the project. I would also like to thank Stewart Craig and Hannah Agate, the dockmaster at the MIT Sailing Pavilion, for allowing me to use their facilities for experimentation. Finally, I would like to thank my old phone for collecting GPS data and which due to an unfortunate accident during data collection is now at the bottom of the Charles River.

REFERENCES

[1] Popper, A. N., and Hawkins, A. D., 2019, "An Overview of Fish Bioacoustics and the Impacts of Anthropogenic Sounds on Fishes," J. Fish Biol., **94**(5), pp. 692–713.

[2] Petroni, A., Biagi, M., Colonnese, S., Cusani, R., and Scarano, G., 2015, "Vessels Traffic Estimation through Image Processing Applied to Acquisitions by Hydrophones," *OCEANS 2015 - Genova*, pp. 1–4.

[3] 2012, "What Is a Hydrophone?," AZoSensors.com [Online]. Available: https://www.azosensors.com/article.aspx?ArticleID=13. [Accessed: 27-Sep-2021].

[4] Vračar, M. S., and Mijić, M., 2011, "Ambient Noise in Large Rivers (L)," J. Acoust. Soc. Am., **130**(4), pp. 1787–1791.

[5] Pollara, A., Sutin, A., and Salloum, H., 2017, "Passive Acoustic Methods of Small Boat Detection, Tracking and Classification," *2017 IEEE International Symposium on Technologies for Homeland Security (HST)*, pp. 1–6.

[6] Gu, J.-E., Jung, S. H., Kang, J., and Woo, H., 2018, "Analysis for Underwater Sound on Natural River Habitat," E3S Web Conf., **40**, p. 02047.

[7] Martin, S. B., and Popper, A. N., 2016, "Short- and Long-Term Monitoring of Underwater Sound Levels in the Hudson River (New York, USA)," J. Acoust. Soc. Am., **139**(4), pp. 1886–1897.

[8] Bureau of Ocean Energy Management Gulf of Mexico OCS Region, 2014, "Appendix J Fish Hearing and Sensitivity to Acoustic Impacts," *Mid-Atlantic and South Atlantic Planning Areas Final Programmatic Environmental Impact Statement*, U.S. Department of the Interior.

[9] McCormick, M. I., Fakan, E. P., Nedelec, S. L., and Allan, B. J. M., 2019, "Effects of Boat Noise on Fish Fast-Start Escape Response Depend on Engine Type," Sci. Rep., **9**(1), p. 6554.

[10] Popper, A. N., and Hawkins, A. D., 2019, "An Overview of Fish Bioacoustics and the Impacts of Anthropogenic Sounds on Fishes," J. Fish Biol., **94**(5), pp. 692–713.

[11] 2016, "17.3: Speed of Sound," Phys. Libr. [Online]. Available: https://phys.libretexts.org/Bookshelves/University_Physics/Book%3A_University_Physics_(OpenStax)/Book%3A_University_Physics_I_-_Mechanics_Sound_Oscillations_and_Waves_(OpenStax)/17%3A_Sound/17.03%3A_Speed_of_Sound. [Accessed: 26-Sep-2021].

[12] Wilson, J. K., “Maritime Surveillance Using a Wideband Hydrophone,” p. 70.
[13] Fischell, E. M., Kroo, A. R., and O’Neill, B. W., 2020, “Single-Hydrophone Low-Cost Underwater Vehicle Swarming,” IEEE Robot. Autom. Lett., **5**(2), pp. 354–361.
[14] Ostrowski, Z., Salamon, R., Kochańska, I., and Marszal, J., 2020, “Underwater Navigation System Based on Doppler Shift – Measurements and Error Estimations,” Pol. Marit. Res., **27**(1), pp. 180–187.
[15] “MITSG Lower Charles Chart” [Online]. Available: https://mit.sea-grant.net/maps/charleschart/. [Accessed: 11-Oct-2021].